

ESTCP Cost and Performance Report



Electromagnetic Induction and Magnetic Sensor Fusion for Enhanced UXO Target Classification

March 2001



ENVIRONMENTAL SECURITY
TECHNOLOGY CERTIFICATION PROGRAM

U.S. Department of Defense

TABLE OF CONTENTS

	Page
1.0 EXECUTIVE SUMMARY	1
2.0 TECHNOLOGY DESCRIPTION	3
2.1 BACKGROUND AND INTENDED USE	3
2.2 TECHNOLOGY DESCRIPTION	3
2.2.1 Mobilization and Operational Requirements	6
2.2.2 Personnel and Training Requirements	7
2.2.3 Health and Safety Training	8
2.3 ADVANTAGES AND LIMITATIONS OF THE TECHNOLOGY	8
3.0 DEMONSTRATION DESIGN	9
3.1 PERFORMANCE OBJECTIVES	9
3.2 SELECTION OF TEST SITE	9
3.3 TEST SITE HISTORY AND CHARACTERISTICS	10
3.4 PHYSICAL SET-UP AND OPERATION	11
4.0 PERFORMANCE ASSESSMENT	13
4.1 REMEDIATION RESULTS	13
4.2 PERFORMANCE DATA	14
4.3 DATA ASSESSMENT	17
4.4 TECHNOLOGY COMPARISON	18
5.0 COST ASSESSMENT	21
5.1 COST ANALYSIS	21
5.2 COST COMPARISON	22
6.0 REFERENCES	25
7.0 POINTS OF CONTACT	27
APPENDIX A: <i>MTADS</i> Target Report from the Final Demonstration	A-1

LIST OF FIGURES

		Page
Figure 1.	Direction and Magnitude of the Magnetic Field Transmitted by the <i>MTADS</i> EM61 Array	5
Figure 2.	Road Map Showing the Location of the Test Site.	10
Figure 3.	Aerial View of the Army Research Laboratory Blossom Point L Range with the Approximate Location of the Demonstration Highlighted.	11
Figure 4.	Example 81-mm Mortar (Left Panel) and 60-mm Mortar (Right Panel) Remediated at the L Range.	13
Figure 5.	Example of Non-Ordnance Remediated at L Range	13
Figure 6.	Two-Dimensional Representation of the Three-Beta Fits for the 81-mm Mortars in the Demonstration	14
Figure 7.	Two-Dimensional Representation of the Three-Beta Fits for Other Targets from the Demonstration Plotted as in Figure 6.	15
Figure 8.	ROC Curve for Detection of 81-mm Mortars.	16
Figure 9.	ROC Curve for Detection of All Ordnance.	16
Figure 10.	Two-Dimensional Representation of the Three-Beta Fits to All Targets Dug in the Demonstration with Ellipses for Each Ordnance Class Derived from the 81-mm Mortar Ellipse.	17
Figure 11.	Results of a Monte Carlo Simulation of Fitted Betas Resulting from a Range of Model 81-mm Mortars with Two Sources of Noise Compared to the Results from the Demonstration.	19
Figure 12.	ROC Curve for Classification Using These Methods Compared to Results Using Magnetic Dipole “Size” and Dipole Orientation.	20

LIST OF TABLES

		Page
Table 1.	Typical Logistics Costs for a 2-week Survey Assuming No Surface Clearance or Remediation.	7
Table 2.	Demonstration Schedule.	11
Table 3.	Size Distributions Used in Magnetometer Analysis of the Demonstration Results	19
Table 4.	Cost Comparison for a Hypothetical 200-Acre Survey Using These Methods.	21

LIST OF ACRONYMS

ARL	Army Research Laboratory
DAS	Data Analysis System Computer
DoD	Department of Defense
EM	Electromagnetic
EOD	Explosives Ordnance Disposal
ESTCP	Environmental Security Technology Certification Program
FA	False Alarm
GIS	Geographic Information System
GPS	Global Positioning System
HAZWOPR	Hazardous Waste Operations
IDA	Institute for Defense Analyses
MTADS	Multi-Sensor Towed Array Detection System
NBS	National Bureau of Standards
NIST	National Institute of Standards and Technology
NRL	Naval Research Laboratory
PD	Probability of Detection
QC	Quality Control
ROC	Receiver Operating Characteristics
RTK	Real Time Kinematic
UXO	Unexploded Ordnance

ACKNOWLEDGMENTS

The Multi-Sensor Towed Array Detection System (*MTADS*) development and initial demonstrations were supported by the Environmental Security Technology Certification Program (ESTCP) Program Office. This program, whose aim was to increase the classification ability of the *MTADS* system, was also supported by ESTCP.

The Naval Research Laboratory has managed all *MTADS* activities. The principal investigator for this program is Dr. H.H. Nelson and Dr. J. R. McDonald is the deputy principal investigator.

We wish to acknowledge the critically important contributions made by AETC, Inc. Tom Bell, Bruce Barrow, and Nagi Khadr were instrumental in the development of the model used in this program and Bernard Puc modified the data analysis system to make use of these methods. We appreciate continual program administrative support by Richard Robertson (Hughes, Associates) and field support by Larry Koppe (GeoCenters, Inc).

Finally, we wish to express our grateful appreciation to Dr. Jeff Marqusee for his unflagging and continual commitment to developing and refining automated UXO detection and remediation technologies. This commitment has led to demonstration and validation of a fully field-hardened prototype and to its transition to the commercial sector where is currently available to provide commercial UXO services and continual improvements of our understanding and ability to make use of *MTADS* data.

Technical material contained in this report has been approved for public release.

1.0 EXECUTIVE SUMMARY

Traditional methods for buried UXO detection, characterization and remediation are labor-intensive, slow and inefficient. A large portion, approaching 70% in some cases, of the total budget of a typical remediation effort is spent on digging targets that do not turn out to be UXO.

The Environmental Security Technology Certification Program, ESTCP, has supported the Naval Research Laboratory in the development of the Multi-sensor Towed Array Detection System, *MTADS*, to address these deficiencies. It is efficient and simple to operate by relatively untrained personnel. It can detect and locate ordnance with accuracies on the order of 15 cm. However, even with careful mission planning and site-specific training there are still significant numbers of non-ordnance targets selected.

Most UXO fit a specific profile: they are long and slender with typical length-to-diameter aspect ratios of four or five. Many clutter items, on the other hand, do not fit this profile. Using EM pulsed-induction sensor data, we have developed a model-based estimation procedure, that relies on exploiting the dependence of the induced field on target size, shape and orientation, to determine whether or not a target is likely to be a UXO item.

These methods were demonstrated in August 1999 at a live test range, the L Range at the Army Research Laboratory's Blossom Point Facility. Towed-array magnetometer (one pass) and EM pulsed-induction data (two orthogonal passes) over the three acre site were collected in 12 survey hours. After analysis of the resulting data sets, 201 targets were classified by their EM response coefficients and flagged for remediation. Target remediation and identification required 12 man-days.

A total of 188 targets were recovered from this test area. There were 66 ordnance items, 20 ordnance related items, 66 exploded fragments, and 36 items not related to ordnance. The ordnance items broke down into three groups: 48 81-mm mortars, 8 mortars of smaller sizes, and 10 miscellaneous ordnance items.

The results of our analysis are presented graphically and ROC curves are derived and compared to the baseline *MTADS* magnetometer analysis. For a single ordnance item, 81-mm mortars, we achieve roughly 60% reduction in false alarms without impacting PD. In order to identify the small fuzes in this field as ordnance, a large number of clutter items have to be included, we are only able to reject ~25%. In part, this is the inevitable result of trying to discriminate ordnance ranging in size from fuzes to 5-in rockets from clutter. This difficulty may be mitigated by obtaining more data, hence better fit statistics, on the smaller ordnance items.

Compared to a traditional "Mag and Flag" survey, these methods cost 25% more on a per acre basis. Considering that "Mag and Flag" surveys only detect ~35% of deeper targets, these methods are far more cost effective on a detected target basis. In addition, the false alarm rejection mentioned above is not applicable to a "Mag and Flag" survey. A careful comparison of these methods to the *MTADS* baseline analysis is planned for Fall 2001 and will be reported.

This page left blank intentionally.

2.0 TECHNOLOGY DESCRIPTION

2.1 BACKGROUND AND INTENDED USE

Buried unexploded ordnance, UXO, is one of the Department of Defense's most pressing environmental problems. Not limited to active ranges and bases, UXO contamination is also present at DoD sites that are dormant and in areas adjacent to military ranges that are under the control of other government agencies and the private sector.

Traditional methods for buried UXO detection, characterization and remediation are labor-intensive, slow and inefficient. Typical detection and characterization methods rely on hand-held detectors operated by explosive ordnance disposal (EOD) technicians who slowly walk across the survey area. This process has been documented as inefficient and marginally effective.¹ In addition, a large portion, approaching 70% in some cases, of the total budget of a typical remediation effort is spent on digging targets that do not turn out to be UXO.

The Environmental Security Technology Certification Program, ESTCP, has supported the Naval Research Laboratory in the development of the Multi-sensor Towed Array Detection System, *MTADS*, to address these deficiencies. The *MTADS* incorporates both cesium vapor full-field magnetometers and EM pulsed-induction sensors in linear arrays that are towed over survey sites by an all-terrain vehicle. Sensor positioning is provided by state-of-the-art Real Time Kinematic (RTK) GPS receivers. The survey data acquired by *MTADS* is analyzed by an NRL-developed Data Analysis System (DAS). The DAS was designed to locate, identify and categorize all military ordnance at its maximum self-burial depth. It is efficient and simple to operate by relatively untrained personnel.

The performance of the *MTADS* has been demonstrated at a number of prepared sites and live ranges over the past two years.²⁻¹¹ It can detect and locate ordnance with accuracies on the order of 15 cm.⁵ However, even with careful mission planning and preliminary training there are still significant numbers of non-ordnance targets selected. Thus, more effective discrimination algorithms are required.

This program was organized on the premise that classification based on shape is central to the problem of discriminating between unexploded ordnance (UXO) and clutter. Most UXO fit a specific profile: they are long and slender with typical length-to-diameter aspect ratios of four or five. Many clutter items, on the other hand, do not fit this profile. Using pulsed-induction sensor data, we have developed a model-based estimation procedure to determine whether or not a target is likely to be a UXO item. The model relies on exploiting the dependence of the induced field on target size, shape and orientation.

2.2 TECHNOLOGY DESCRIPTION

The standard *MTADS* technology has been described in detail previously.¹² Briefly, the system hardware consists of a low-magnetic-signature vehicle that is used to tow linear arrays of magnetometer and pulsed-induction sensors to conduct surveys of large areas to detect buried UXO. The *MTADS* tow vehicle, manufactured by Chenoweth Racing Vehicles, is a custom-built off-road vehicle, specifically modified to have an extremely low magnetic signature. Most ferrous

components have been removed from the body, drive train and engine and replaced with non-ferrous alloys.

The *MTADS* magnetometers are Cs-vapor full-field magnetometers (Geometrics Model 822ROV). An array of eight sensors is deployed as a magnetometer array. The time-variation of the Earth's field is measured by a ninth sensor deployed at a static site removed from the survey area. These data are used to correct the survey magnetic readings. The pulsed-induction sensors (specially modified Geonics EM61s) are deployed as an overlapping array of three sensors. The sensors employed by *MTADS* have been modified to make them more compatible with vehicular speeds and to increase their sensitivity to small objects.

The sensor positions are measured in real-time (5 Hz) using the latest RTK GPS technology. All navigation and sensor data are time-stamped and recorded by the data acquisition computer in the tow vehicle. The DAS contains routines to convert these sensor and position data streams into anomaly maps for analysis.

The standard *MTADS* analysis method has also been described previously.¹³ The magnetometry data has been very successfully modeled using a dipole response. We routinely recover target x,y positions to within 15 cm and target depths to $\pm 20\%$.⁵ Within the signal to noise ratio of the *MTADS*, we see no residual signature attributable to higher moments.¹³ The pulsed-induction modeling has been less successful. The standard algorithm is based on a sphere model and does not well represent the signatures we obtain. We have discussed the deficiencies of this model and proposed an ordnance model based on a prolate spheroid.¹³

This program was organized on the premise that classification based on shape is central to the problem of discriminating between unexploded ordnance (UXO) and clutter. Most UXO fit a specific profile: they are long and slender with typical length-to-diameter aspect ratios of four or five. Many clutter items, on the other hand, do not fit this profile. Using pulsed-induction sensor data, we have developed a model-based estimation procedure to determine whether or not a target is likely to be a UXO item. The model relies on exploiting the dependence of the induced field on target size, shape and orientation.

The EM61 is a time domain instrument. It operates by transmitting a magnetic pulse that induces currents in any nearby conducting objects. These currents produce secondary magnetic fields that are measured by the sensor after the transmitter pulse has ended. The sensor response is the voltage induced in the receiver coil by these secondary fields, and is proportional to the time rate of change of the magnetic flux through the coil. The sensor integrates this induced voltage over a fixed time gate and averages over a number of pulses. An illustration of the magnitude and direction of the field transmitted by the *MTADS* array is shown in Figure 1. Note that the field experienced by an object directly below the array is substantially different than an object in front of or behind the array. This allows us to get several "looks" at the target as we conduct a survey and aids greatly in our model fits.

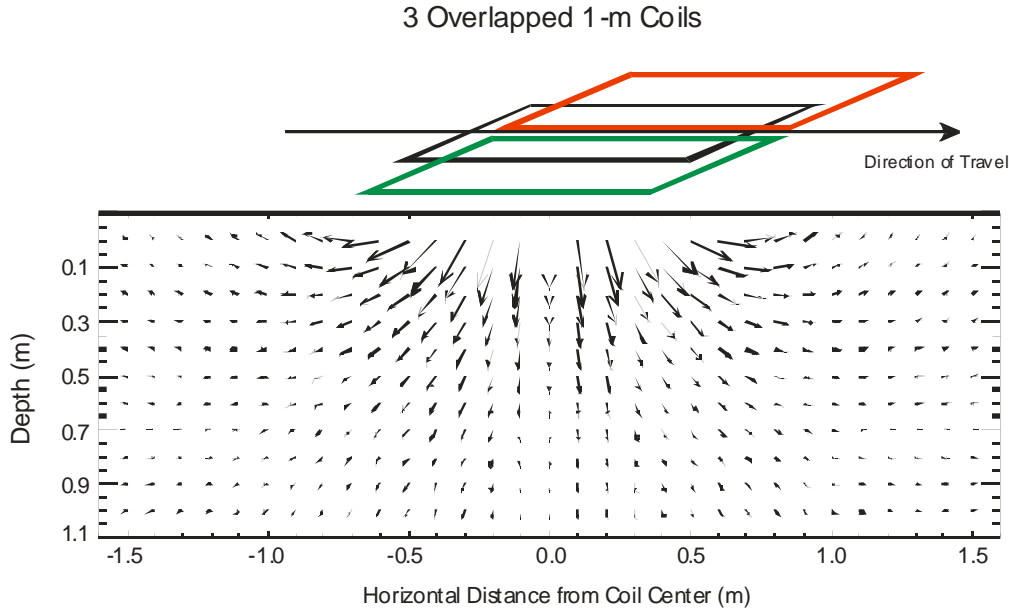


Figure 1. Direction and Magnitude of the Magnetic Field Transmitted by the MTADS EM61 Array.

The model to be used in this demonstration has been jointly developed by NRL and AETC, Inc. and has been described recently.^{14,15} Briefly, it relies upon the fact that the EM61 signal is a linear function of the flux through the receiving coil. The flux is assumed to originate from an induced dipole moment at the target location given by:

$$\mathbf{m} = \mathbf{UBU}^T \cdot \mathbf{H}_0$$

where \mathbf{H}_0 is the peak primary field at the target, U is the transformation matrix between the coordinate directions and the principal axes of the target, and B is an empirically-determined, effective magnetic polarizability matrix. For any arbitrary compact object, this matrix can be diagonalized about three primary body axes and written as:

$$B = \begin{bmatrix} \beta_x & 0 & 0 \\ 0 & \beta_y & 0 \\ 0 & 0 & \beta_z \end{bmatrix}.$$

The relative magnitudes of these β 's are determined by the size, shape, and composition of the object as well as by the transmit pulse and fixed time gate of the EM61. Different time gates may result

in different values and different relative values of these β 's for a given object. The transformation matrix contains the angular information about the orientation of these body axes.

For an axisymmetric object, B has only two unique coefficients, corresponding to the longitudinal (β_l) and transverse (β_t) directions:

$$B = \begin{bmatrix} \beta_l & 0 & 0 \\ 0 & \beta_t & 0 \\ 0 & 0 & \beta_t \end{bmatrix}$$

Empirically, we observe that for elongated ferrous objects such as cylinders and most UXO, the longitudinal coefficient is greater than the transverse coefficient. For flat ferrous objects such as disks and plates, the opposite is true. This matches the behavior of these objects in the magnetostatic limit. For non-ferrous objects such as aluminum cylinders and plates, these relationships are reversed.

We tested several implementations of this model in our early shakedown demonstrations. All were designed to take advantage of the fact that we obtain reliable position (x,y,z) information from the magnetometer signals. We then fitted the pulsed-induction response to models with combinations of two or three response coefficients, β , and two or three orientation angles. One of the goals of these shakedown demonstrations was to determine which of these models resulted in the most classification utility with the least data collection expense. As we will discuss below, we have determined that conducting two orthogonal EM surveys and fitting the data using the three β , three angle model yields the optimum results. This survey methodology was used in this Demonstration.

2.2.1 Mobilization and Operational Requirements

All *MTADS* equipment is designed to be transported to field sites to support survey and remediation operations. All electronic instrumentation and office equipment is equipped with foam-padded containers that can be shipped by air or truck. All field equipment is designed to be transported by a tractor-trailer. We pack and transport an extensive list of spare equipment and components for field repair and replacement. Small electronics and mechanical repair stations are packed and resupplied before each deployment. We have dedicated communications and two-way radio equipment to support the field operations. Battery charging stations are carried to support all radios, electronics, and navigation equipment.

We mobilize to survey sites using a rented tractor-trailer. This rental is economical enough that the rig is typically left on site throughout the survey for storage of spares. All *MTADS* equipment required for a mag and EM survey can be accommodated in a 50-ft trailer. At some sites, electrical power, water, and office facilities are available to support our operations. More typically, one or several of these are not available on-site and are leased and delivered to the site before *MTADS* operations begin. Typical logistics support requirements and their rental costs are shown in Table 1.

Table 1. Typical Logistics Costs for a 2-week Survey Assuming No Surface Clearance or Remediation.

Activity	\$K	\$K
Presurvey Expenses		
Initial Site Visit	3.0	
Establish Navigation Control Points	6.0	
Draft Demonstration Plan & Health and Safety Work Plan	15.0	
Presurvey Total		24.0
Equipment Transport		
Truck Rental	3.5	
Fuel/Permits/Tolls	1.0	
Driver	1.5	
Subtotal for Equipment Transport		6.0
On-site Logistics		
Office Trailer	3.0	
Electrical Hookup	1.0	
Portable Toilets	1.0	
Power Generator/Fuel	3.5	
Tent for Equipment Repair	1.5	
Subtotal for On-site Logistics		10.0
Total		40.0

2.2.2 Personnel and Training Requirements

MTADS surveys to date have been overseen by a Senior Research Scientist. Although, in the strictest sense, this results in an over-qualified field supervisor, we find it to be an efficient deployment of resources. Small problems are avoided or solved more quickly and our total productivity is higher with a senior supervisor. In a commercial environment, where survey jobs are more frequent and of longer duration, this senior supervisor may only be required on site for the first few days of the survey and after that, to be available for telephone consultation.

The field operations/data collection are carried out by a single vehicle operator who doubles as the site safety officer. Because of this dual role, we employ a retired EOD technician for this position. If a site has a separate safety officer, the requirements for vehicle operator would be a standard geophysical field technician. Survey guidance, reorienting the driver after turns, and general maintenance and housekeeping are provided by 3-5 laborers from the local labor pool. On most sites, these laborers are required to be hazardous waste operations (HAZWOPR) certified.

MTADS demonstration surveys have all been carried out with simultaneous or overlapping remediation operations. This requires the presence of experienced data processing and data analysis personnel on-site. If remediation is to be accomplished at a later date, only a BS-level data analyst is required on-site for QC purposes. In this case, the trained analyst can work from home base. One of the goals of this project is to make the data analysis more routine so that less-trained employees can be productive. We have made some progress in this direction but have not succeeded completely.

When working on live ranges or former bombing or gunnery targets, we routinely conduct a walkover and surface clean prior to conducting vehicular surveys. The surface walkovers are carried out by subcontractor UXO-certified specialists. The typical team consists of one UXO-certified supervisor and five laborers. Depending on the circumstances, the laborers either have HAZWOPR certification or are trained on-site by the UXO supervisor.

2.2.3 Health and Safety Training

As mentioned above, many of the workers on a survey are required to have HAZWOPR and/or UXO-certification. In addition, a complete Health and Safety Work Plan is required on all UXO operations. This work plan contains detailed descriptions of the hazards expected on site, standard procedures for identifying these hazards and protocols for dealing with them, and emergency health care procedures.

2.3 ADVANTAGES AND LIMITATIONS OF THE TECHNOLOGY

We have demonstrated^{5,7} that an impressive level of discrimination is possible using the baseline *MTADS* if a small training area is investigated prior to data analysis on the entire site and if the distribution of ordnance types is limited. This discrimination is based primarily on fitted dipole “size.” In this program we have demonstrated methods designed to add an extra “dimension” to the discrimination, that of “shape.” For items with similar induced magnetic dipoles we can discriminate based on the ratio of responses along the item's three axes to the EM induction sensors in the *MTADS* suite. As we show in a later section, this adds some discrimination capability to the system.

Even with the most optimistic result however, these methods will not result in a perfect system. As we have stated above, this program is based on the idea of classification by shape. By definition, this implies that clutter items that have similar shapes to ordnance will be classified as ordnance. Items such as pipes and post sections are representative of this problem. If it is important to reduce remediation costs to the extent that these items are not dug, other methods, possibly sensitive to composition or the presence of explosive compounds, will have to be employed in conjunction with those developed in this program.

3.0 DEMONSTRATION DESIGN

3.1 PERFORMANCE OBJECTIVES

The objective of the Demonstration was to quantify the classification performance available using commercially-available pulsed-induction sensors and the data modeling algorithms developed in this program. The Demonstration proceeded in three phases: data collection, data analysis, and target marking and remediation.

Data collection consisted of surveying an approximately three-acre area on a live range, known to have had many detonations, using magnetometers and pulsed-induction sensors. The magnetometer survey was conducted in an E-W orientation to minimize the effects of vehicle self-signature. The pulsed-induction survey was carried out both E-W and N-S to get the best possible “illumination” of each target.

Data were analyzed using the *MTADS* Data Analysis System modified to include the 3- β approach. This upgrade allows simultaneous analysis of a magnetometer and several pulsed-induction survey data sets. The analysis consists of fitting individual target signatures to the model described above to extract target position, size and relative response coefficients along three orthogonal axes. We planned to select approximately 200 targets for remediation. After analysis of the survey data we found that there were only ~200 targets in the survey area with signatures well enough separated to get a good model fit so no further selection was necessary. This target set represents ~25% of those targets with magnetic anomaly > 50nT and/or EM anomaly > 70mV. In our view, this is a large enough fraction of the total targets to ensure that a representative sample of all targets was remediated. The relative fitted response coefficients were used to classify the target as UXO or scrap. This resulted in a spreadsheet-like target report that included target number, location, depth and predicted class. This spreadsheet, and the reasoning behind the target assignments, was communicated to personnel from the Institute for Defense Analyses (IDA) before digging the selected targets.

The final phase of the Demonstration consisted of flagging and digging the selected targets by a commercial UXO firm. Careful remediation notes were made for each target that included actual target location, field identification of the target, rough target dimensions, and a photograph of each target. These field results, in conjunction with the fitted target responses, provided the basis for quantitative evaluation of this method's classification performance. Later sections of this report will present these results in detail.

3.2 SELECTION OF TEST SITE

The site of this Demonstration, the L Range at the Army Research Laboratory's Blossom Point Facility, was chosen to be a realistic test of the methods developed in this program. The range has been used for a variety of mortar and barrage rockets and contains large amounts of clutter and scrap. The preliminary testing in this program was conducted on a test field with mostly ordnance and ordnance-simulants which were appropriate for model development but not particularly representative of a live-site situation. This range is a good model site for demonstrating this technology.

3.3 TEST SITE HISTORY AND CHARACTERISTICS

During World War II, Harry Diamond and his team at the National Bureau of Standards (NBS, now named NIST) needed open areas where they could test the fuzes they were developing. They established test sites at Aberdeen Proving Ground, MD, Fort Fisher, NC, and, in early 1943, NBS leased land and established a proving ground for proximity fuzes at Blossom Point. By September 1945, 14,000 rocket and mortar rounds had been fired. In 1953, the lease on the property was transferred to the Army, which operated the property as a fast-reaction, low-cost range for experimental work. Firing ranges provided a 2000-yard maximum range for land impact and a 10,000-yard maximum for water impact. During the Vietnam War, the Army's Harry Diamond Laboratory was very active at the site.

The L Range is the main range for impact testing of various munitions at Blossom Point. It is approximately 800 feet wide by 5000 feet long and encompasses ~93 acres. This range has been the primary impact area throughout the history of the site. Some of the known firings include 81-mm mortars in 1961, 2.75-inch rockets fired from helicopters throughout the 1970's, a variety of experimental 60-mm mortars, 75-mm projectiles, 81-mm mortars and various barrage rockets.

HFA, Inc. conducted an ordnance removal at the Blossom Point Test Facility in 1996.¹⁶ Two sites were cleared in conjunction with utility work and construction. Two sites totaling 66 acres were cleared; one a clear area parallel to L Range and one a wooded area north of the first. Targets were dug to 4 feet on the construction sites and 2 feet for the utility easements. Seven hundred fifty three UXO items and 9,267 lbs. of scrap were removed from the site. The UXO included a wide variety of ordnance types and classes with a preponderance of 20- and 30-mm rounds, 60- and 81-mm mortars, and 4.2-in rockets. This is consistent with the firing records.

Figure 2 is a road map of a portion of Charles County, Maryland showing the location of Blossom Point relative to La Plata, the County Seat. The ARL Blossom Point Facility is classified as a range, and as such is closed to the public. Access to DoD employees and contractors is limited by the operating hours of the facility. Figure 3 is an aerial photo of the Blossom Point Field Facility with the area comprising the Final Demonstration test site highlighted in yellow.

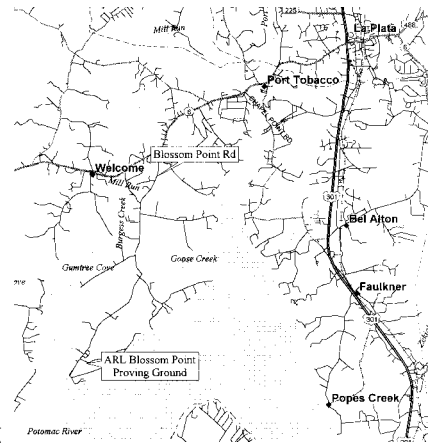


Figure 2. Road Map Showing the Location of the Test Site.

The Demonstration area is located on high ground, well above the surrounding rivers. The site has good sky view for GPS but is bordered by a densely wooded area that is ideal for testing non-GPS location systems. This Demonstration was carried out in the GPS-accessible portion of the site.



Figure 3. Aerial View of the Army Research Laboratory Blossom Point L Range with the Approximate Location of the Demonstration Highlighted.

3.4 PHYSICAL SET-UP AND OPERATION

Since this Demonstration was conducted on the Blossom Point site adjacent to where our equipment is housed, many of the normal pre-survey logistics listed in Table 1 such as establishment of first-order GPS markers, transport of the equipment to the site, and equipment setup and testing were not required. We performed the Demonstration "out of the garage." In all other ways, this Demonstration was conducted in accordance with our normal survey practices. Table 2 provides the actual demonstration schedule.

Table 2. Demonstration Schedule.

Date	Activity	Required Time
29 July 1999	Magnetometer survey of site	2 hrs survey time
3 August 1999	East-West EM survey of site	5 hrs survey time
4 August 1999	North-South EM survey of a portion of the site Data analysis and target classification	1 hr survey time
12-13 August 1999	Flag targets for remediation	4 hrs survey time
16-18 August 1999	Target remediation	16 man-hours
26 August 1999	Required demolition. 81 shot on 73 targets	12 man-days

This page left blank intentionally.

4.0 PERFORMANCE ASSESSMENT

4.1 REMEDIATION RESULTS

After completion of the magnetometer and two EM surveys in perpendicular directions, 201 targets were analyzed and marked for remediation on the L Range Final Demonstration site. A total of 188 targets were recovered from this test area, 13 were dry holes. Examples are pictured in Figures 4 and 5. There were 66 ordnance items, 20 ordnance-related items (rocket motors with fins and mortar tail booms), 66 exploded fragments, and 36 items not related to ordnance. The ordnance items broke down into three groups: 48 81-mm mortars, 8 mortars of smaller sizes, and 10 miscellaneous ordnance items. The miscellaneous items included 2 bomb fuzes, a 76-mm projectile, and two 5-in rockets. The exploded fragments appeared to be mostly from mortar casings. The non-ordnance items included cable tie down points for test towers that had been removed, block and tackles from the cables, and a variety of odd scraps of metal (rebar, sheet metal, angle iron, and bolts).



Figure 4. Example 81-mm Mortar (Left Panel) and 60-mm Mortar (Right Panel) Remediated at the L Range.



Figure 5. Example of Non-Ordnance Remediated at L Range.
(This item is part of a block and tackle used for guy-cables for a test tower.)

An abbreviated version of the *MTADS* target report for these items is attached as Appendix A. Included in this report are the results of the magnetometer and 3β analyses and the field notes on the identity of the remediated items. As the goal of this Demonstration was to validate the utility of the 3β analysis for target classification, all remaining discussion focuses on that analysis.

4.2 PERFORMANCE DATA

We will concentrate our initial discussion on the 81-mm mortars as they provide the best fit statistics. The results of the three-beta fits for the 81-mm's are shown in Figure 6. The value of the primary beta (largest) is plotted on the abscissa. The two smaller betas are plotted on the ordinate, where the symbol in the plot is the average and the vertical line represents the spread between the two values. We find this to be an easier way to visualize the spread in the data than plotting the points in three dimensions. Note that if the fit results were perfect (no measurement errors) then the data would all be symbols with no vertical line (secondary betas are equal for axisymmetric objects). In the Final Report¹⁷ for this program we detailed results from bench tests that confirm this.

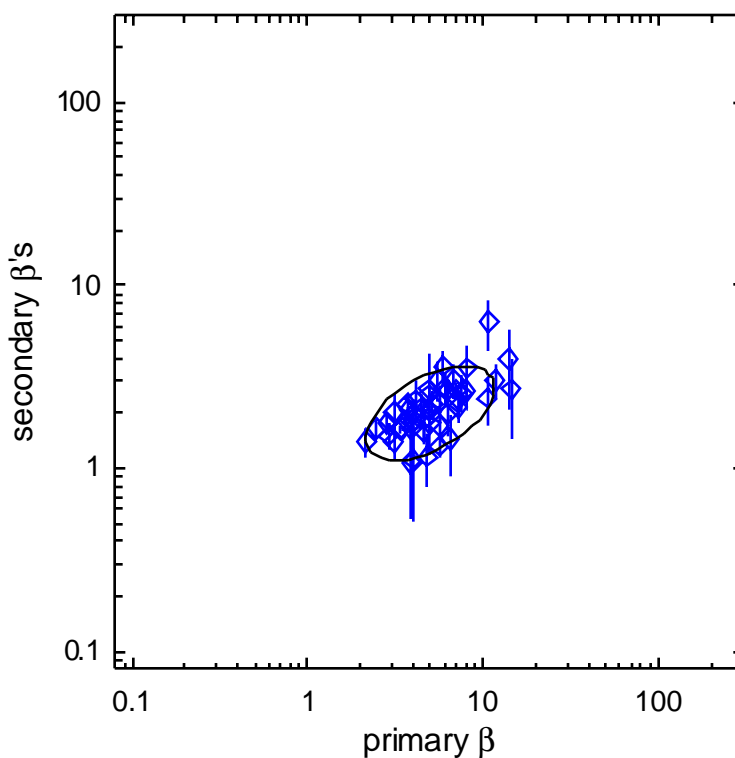


Figure 6. Two-Dimensional Representation of the Three-Beta Fits for the 81-mm Mortars in the Demonstration. (The value of the primary beta (largest) is plotted on the abscissa and the two smaller betas are plotted on the ordinate with the symbol representing the average and the vertical line the spread.)

The three beta values for the 81-mm mortars are best described by a log-normal distribution. In logarithmic quantities, the mean is 0.697, 0.318, and 0.310 with standard deviations of 0.2, 0.09, and 0.13 for β_1 , β_2 , and β_3 respectively. In measured units, this corresponds to an average response of 4.98 along the length of the mortar and 2.0 transverse to this. Note that the values range from 2 to 12 along the primary axis, which is much greater than the 20-30% observed in preliminary testing for objects in our test field. It is thought that this enlarged spread is largely due to positioning errors in height as the array is towed over the uneven ground of a live site. We will discuss this point in more detail later in the report. The ellipse plotted in Figure 6 represents a three dimensional ellipsoid with major and minor radii that are equal to two standard deviations of the primary and secondary betas. The ellipse is tilted because of a weak correlation between the primary versus the secondary betas (stronger primary betas correlate with stronger secondary betas). As we will show below, this ellipsoidal curve can be used to calculate the probability that a given beta fit represents an 81-mm mortar.

The three beta fit results for the other ordnance items recovered at the L Range are plotted in the left panel of Figure 7. The approximate primary versus secondary beta values range from 0.7/0.5 for the bomb fuse to 178.0/62.0 for the 5-in rockets. A similar plot for the fragments, the ordnance related scrap, and the non-ordnance scrap is presented in the right panel of Figure 7. It is interesting to note that the bulk of the fragments do not overlap the 81-mm mortars. One would expect that a large spread in the secondary betas should result from an irregularly shaped object. Overall, the spread observed in the right panel of Figure 7 is not much greater than the spread for the axisymmetric ordnance objects (Figure 6 and left panel of Figure 7). After examining photos of the objects dug, this is not too surprising. Most of the scrap, to first order, is elongated, with approximately equal secondary dimensions.

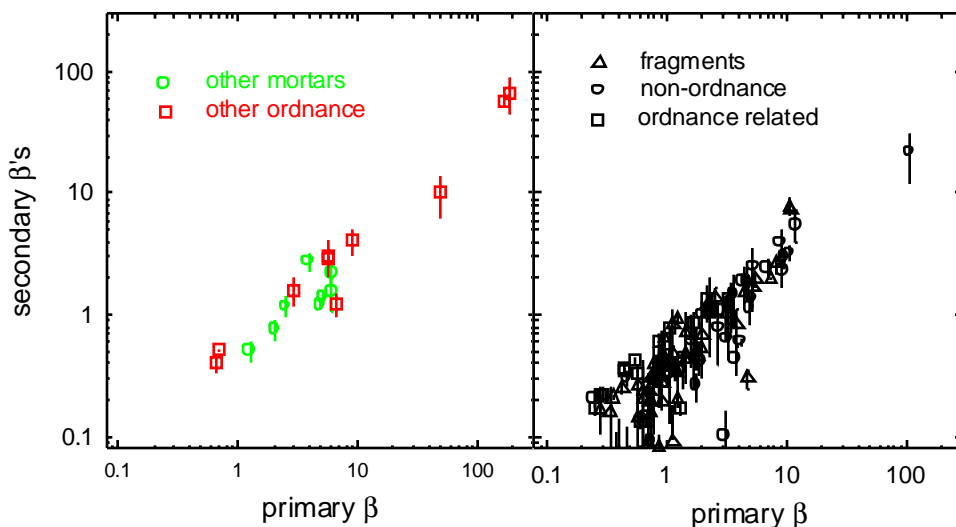


Figure 7. Two-Dimensional Representation of the Three-Beta Fits for Other Targets from the Demonstration Plotted as in Figure 6.

Examples of ROC curves based on the L Range data are shown in Figures 8 and 9. To generate these curves, the ellipsoid in Figure 6 is expanded (in three dimensions) and the number of ordnance (PD)

and non-ordnance (FA) beta values that fall within this three dimensional region are counted. Figure 8 plots the results for a single 81-mm ellipsoid. In Figure 9, ellipsoids are generated about each of the ordnance items present. The sizes of these ellipsoids are expanded uniformly based on the standard deviations and correlations of the 81-mm betas; too few of these other ordnance items were fitted to generate valid beta statistics. This is illustrated on the familiar beta plot in Figure 10.

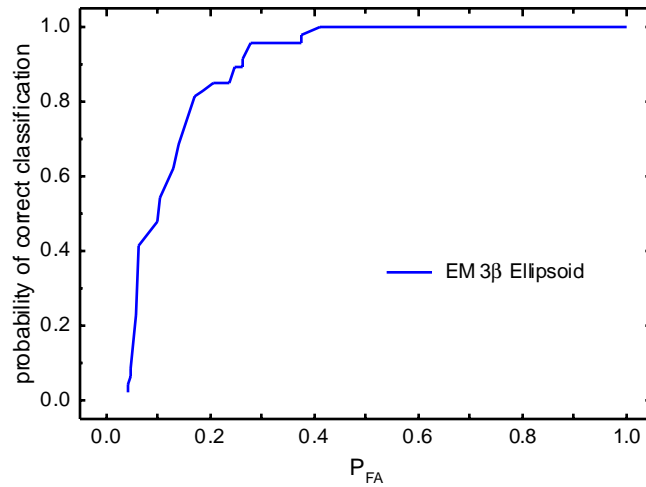


Figure 8. ROC Curve for Detection of 81-mm Mortars.

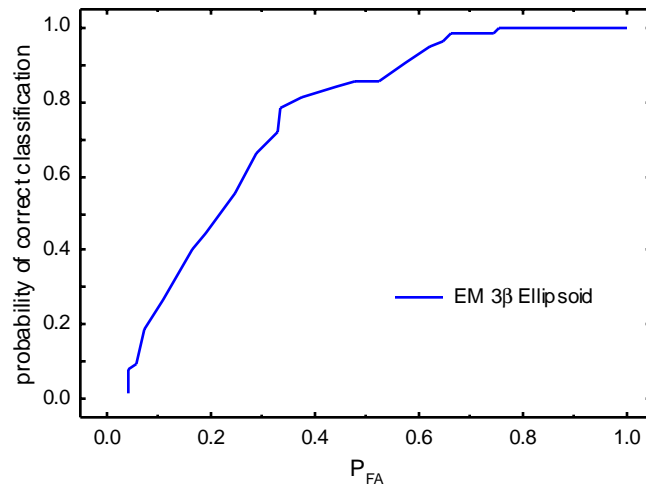


Figure 9. ROC Curve for Detection of All Ordnance.

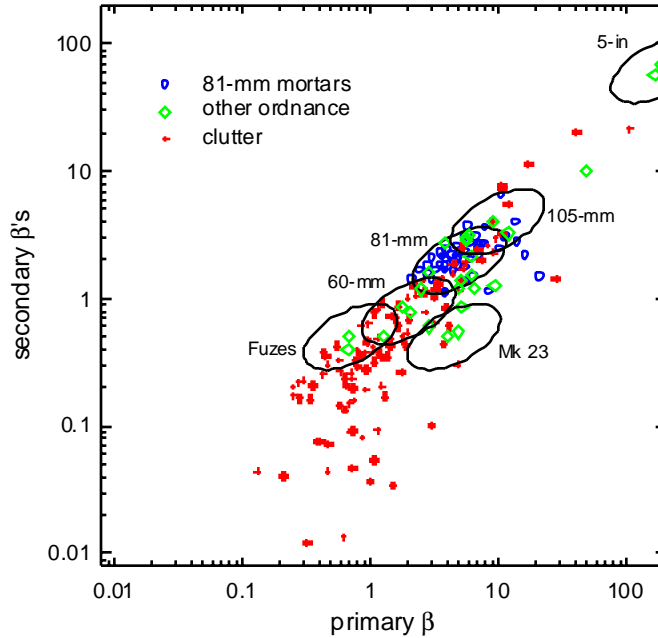


Figure 10. Two-Dimensional Representation of the Three-Beta Fits to All Targets Dug in the Demonstration with Ellipses for Each Ordnance Class Derived from the 81-mm Mortar Ellipse.

The discrimination performance we achieve for a single ordnance item, 81-mm mortars, matches results we have obtained in earlier, controlled tests of this method. We achieve a roughly 60% reduction in false alarms without impacting P_D . The story is more complicated when trying to discriminate several classes of ordnance from the background clutter, Figure 9. We still reduce false alarms by 25%, but in order to identify the small fuzes in this field as ordnance, a large number of clutter items have to be included. In part, this is the inevitable result of trying to discriminate ordnance ranging in size from fuzes to 5-in rockets from clutter. This difficulty may be mitigated by obtaining more data, hence better fit statistics, on the smaller ordnance items. Using the error ellipsoid derived from the distribution of 81-mm mortar fits, as we were forced to do, may well overstate the region of the 3-D space occupied by the smaller ordnance items. As we obtain more model fits to remediated ordnance and improve our fit statistics we will be able to test this premise.

4.3 DATA ASSESSMENT

The survey data collected during this Demonstration were of sufficient quality to meet the stated goals. We were able to increase the discrimination available using *MTADS* EM induction survey data for targets with isolated signatures. Several features of the data limited the classification ability, however. We showed in the earlier controlled tests that sensor noise and sensor location error limited the estimated betas to a precision of $\sim 25\%$. Some improvement is possible in this regard, but not a lot. The GPS units used for sensor location on the *MTADS* array are state-of-the-art receivers with cm-level precision. Because of the response of the EM61 sensors to the GPS antenna, the antenna is located ~ 1.5 m in front of the sensor array. Although the antenna location is known to centimeters, there is some location uncertainty introduced by the back projection of the sensor

locations from the antenna position. A two-antenna array, with a GPS antenna in front of and behind the EM sensors, would reduce sensor location uncertainties. At the time of this Demonstration, this would have involved the purchase of another independent GPS receiver/radio combination. Now, because of the demand from the mining and construction markets, dual antenna systems are available for a modest increase in price. Sensor noise is a different issue. Progress here requires a new generation of EM induction sensors.

Compared to the data collected during our initial, controlled tests, there was a decrease in the precision of the fitted beta values during this Demonstration. We attribute this to vertical motion of the EM array over the rough ground at the live site. In an attempt to provide some quantitative underpinning to this assertion, we have performed a Monte Carlo simulation of the fitted response of an 81-mm mortar simulant with varying sources of noise. The object used in the simulation had betas of 5,2,2, about that expected for an 81-mm mortar. The object was placed at a distance of 0.6 m from the sensor array and given a random x,y position relative to the survey tracks and a random orientation. Each simulation included real *MTADS* GPS and sensor noise. The results of this simulation are shown in Figure 11. The top panel shows the results using only GPS and sensor noise. In this case, the fitted betas exhibit just the precision observed in controlled tests, ~25%. For the simulation depicted in the bottom panel of Figure 11, a component of sensor height variation was added to simulate array bouncing over rough ground. We find that red noise with an RMS amplitude of 3 cm reproduces the spread in betas observed in the Demonstration. This is easily within the realm of possibility; the *MTADS* EM array platform does not have a suspension and is observed to bounce in rough terrain.

The terrain at the L Range demonstration was not especially rough for a live-site demonstration; *MTADS* has been demonstrated at several sites with much more challenging terrain. Therefore, to take advantage of the shape information inherent in the response of targets to the EM61 array, better control of vertical sensor displacements will be required. One option is to add suspension to the array platform. Another, possibly more effective, method would be to record the displacements of the array using inertial sensors and explicitly account for the position of the array in three dimensions in the data analysis procedure.

4.4 TECHNOLOGY COMPARISON

The obvious baseline for comparison of the value of the technology demonstrated here is the current *MTADS*. As mentioned above, the baseline *MTADS* is able to achieve a reasonable level of discrimination using magnetometry fits alone, especially when the ordnance distribution is limited. We will thus compare the results obtained in this demonstration with those that would be obtained by *MTADS* at the same site. To accomplish this, we have made use of the fitted magnetometer "size" parameter that is included in the target report in Appendix A. For each ordnance class, we calculate a mean "size." Just as in the case of the 3-beta algorithm, we are able to calculate a distribution about this mean for the 81-mm mortars. We use the 81-mm size distribution to generate a proportionally-sized distribution for each ordnance class. The distributions derived are listed in Table 3.

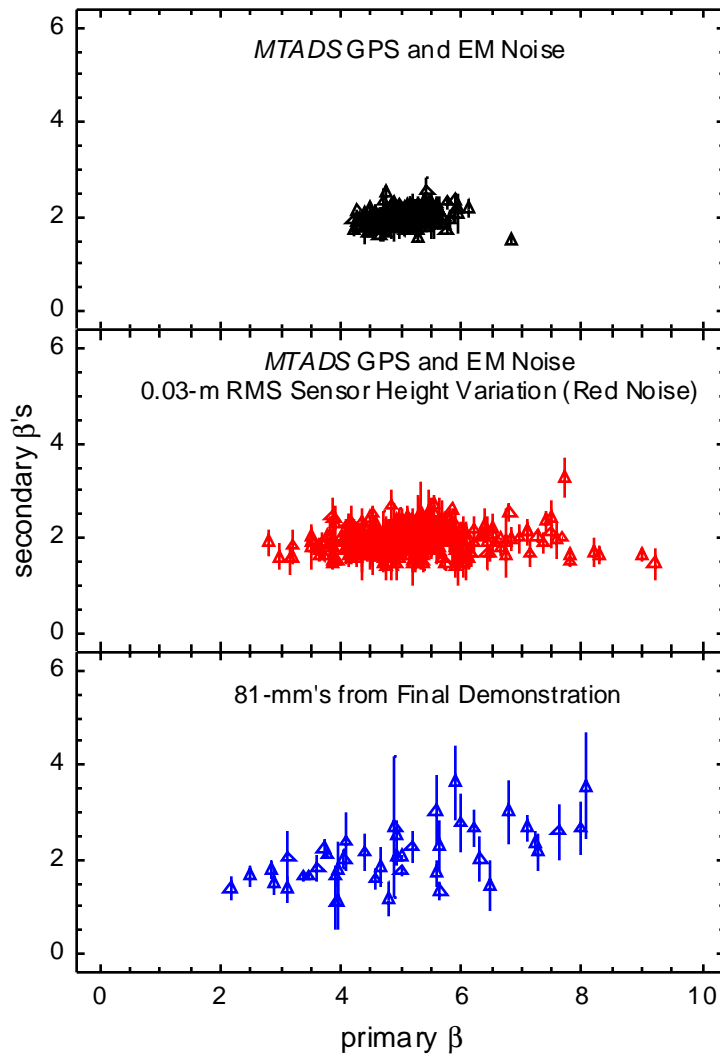


Figure 11. Results of a Monte Carlo Simulation of Fitted Betas Resulting from a Range of Model 81-mm Mortars with Two Sources of Noise Compared to the Results from the Demonstration.

Table 3. Size Distributions Used in Magnetometer Analysis of the Demonstration Results.

Ordnance Class	Size Distribution (mm)	Ordnance Class	Size Distribution (mm)
Fuzes	43 ± 9	81-mm mortar	76 ± 16
Mk23	56 ± 11	105-mm projectile	105 ± 21
60-mm mortar	60 ± 12	5" rocket	212 ± 42

We can then generate a ROC curve for this method by varying the width of the distribution around each ordnance class and declaring each target as ordnance (within the six size bands) or clutter. The result of this analysis is plotted in Figure 12. Also plotted in the Figure is a curve generated by enhancing the magnetometry analysis by taking advantage of the fitted magnetic dipole orientation for each target. This enhancement relies on the observation that UXO targets have, in general, been shock demagnetized by their impact with the ground and only exhibit induced magnetic moments while fragments and clutter have remanent moments. This was the case for the ordnance recovered at the LRange, only one of the 73 items considered had a magnetic dipole orientation not consistent with an induced dipole only. Note that this method does not automatically eliminate all items with a remanent moment, only those whose net dipole orientation is outside that expected from an item with an wholly induced dipole.

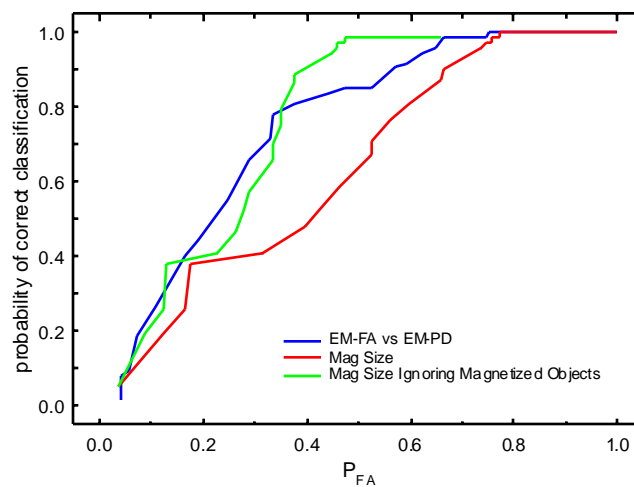


Figure 12. ROC Curve for Classification Using These Methods Compared to Results Using Magnetic Dipole “Size” and Dipole Orientation.

The magnetic dipole “size” suffers from many of the same problems as the 3-beta algorithm when attempting to discriminate all ordnance. In order to capture the fuzes, a large number of small frag items must be included. The magnetic dipole orientation filter helps greatly in this regard as a good number of the frag items are magnetized and are thus correctly identified as clutter.

It is difficult to compare the performance of the analysis of EM61 data presented here with that of other sensors and analysis methods. As we have shown, the current procedure gives excellent results in the test jig and reasonable results at our Test Field, which is a smooth, clean, and level site. The only legitimate comparison is to results obtained by competing technologies on live-site surveys. As these data become available, direct comparisons will follow.

5.0 COST ASSESSMENT

5.1 COST ANALYSIS

The estimated costs for an *MTADS* EM survey in two, orthogonal directions and the data analysis required to implement the model described here for a hypothetical 200 acre survey are listed in Table 4 along with an estimate for a “Mag and Flag” survey of the same area. For neither survey do we assume remediation of targets. The *MTADS* survey has been carried through target analysis providing target maps and target tables with position size and depth of all targets. The “Mag and Flag” survey is assumed to flag each target as it is detected and later survey in the flags for archival purposes.

Table 4. Cost Comparison for a Hypothetical 200-Acre Survey Using These Methods.

Expense		<i>MTADS</i> EM Survey 25 Survey Days		“Mag and Flag” 14 Field Days	
Labor Category	Burdened Rate (\$/hr)	Site#	Total \$	#	Total \$
Site Supervisor	\$100	1	\$20,000		
UXO Site Supervisor	\$70	1		1	\$7,840
Data Analyst	\$60	1	\$12,000		
UXO Supervisor	\$60	1	\$12,000	2	\$13,440
HAZWOPR-Trained Staff	\$25	1	\$5,000		
UXO Specialists	\$30			8	\$26,880
Local Field Support	\$20	4	\$16,000		
Total Labor Cost			\$65,000		\$48,160
Travel @ \$1000/person			\$4,000		\$11,000
Hotel @ \$75/day			\$9,900		\$14,850
Per Diem @ \$45/day			\$5,940		\$8,910
Logistics			\$40,000		\$3,000
Amortization @ \$100/survey hour			\$20,000		
Surveying Flagged Targets for GIS					\$30,000
Total Survey Cost			\$144,840		\$115,920

Based upon our experience in supporting and using the *MTADS* at previous demonstrations, we propose to amortize \$400K of the *MTADS* hardware costs based upon a schedule of 4000 hours of surveys.¹² This is a conservative estimate based on breakage, maintenance, and replacement costs for the past four years.

In our experience with *MTADS* at field operations we have always had one senior scientist/supervisor on site supporting the operation. In addition, we have provided extensive logistics support such as tents for maintenance work, offices with bench spaces for repairs and onsite office spaces for computers and DAS support equipment. It is our experience that these support elements have a positive impact on our survey efficiency and on the quality of the data collected and the on-site analysis product. For this reason, we use the same support and logistics costs for the comparison purposes. A commercial firm in a cost-competitive environment might forgo some of these logistics costs.

The *MTADS* survey costs include two orthogonal EM surveys only; no magnetometer survey is included. If large, deep targets were expected a magnetometer survey would be required and an additional \$50K would be necessary. Since two orthogonal EM surveys are included in the estimate while only one would be required for target detection, it is clear that the added cost of these methods is \$300 per acre. This is approximately equal to the costs required to remediate one or two targets per acre. Thus, the economic breakeven point for the use of these methods is reached when three false alarms per acre are avoided.

For the Mag and Flag operations, we assume that the number of personnel are put on site that can complete the survey in a three week period of performance. This minimizes the travel and logistics costs. The labor mix of UXO technicians to UXO supervisors and the site supervisor support and logistics support are typical of those that we have had quoted to support operations and also factor in information about labor rates and labor mixes typically quoted for operations similar to these.

5.2 COST COMPARISON

These calculations, which show that the methods demonstrated here are 25% more costly on a per acre basis, do not address the ultimate goal of a particular survey, i.e., is the survey being conducted to support remediation activities, or simply to provide an indication of whether the site is contaminated and the extent of the ordnance contamination? Previous studies of the detection efficiencies of mag and flag operations have shown that (at least for sites where ordnance exists below 1 meter in depth), the majority of ordnance remains undetected.

Assuming that the survey is in support of a remediation activity, the cost per detected target is a useful comparison. Using documented mag¹ and flag detection efficiencies of 35%, we find that these methods are more than twice as cost efficient at flagging ordnance for remediation. It should also be noted that following remediation based upon a "Mag and Flag" survey, 65% of the ordnance targets remain in the ground.

Even these numbers do not take into account the false alarm reduction demonstrated in this survey. In the worst-case scenario, discriminating ordnance ranging from fuzes to 5-in shells from scrap, we were able to reject >20% of the false alarms without missing an ordnance target. With a more restricted target set, false alarm reductions of 33 - 50% are possible. Since a "Mag and Flag" survey has no significant classification ability, all targets have to be remediated.

The true cost comparison of interest is a comparison of the results demonstrated by this method vs the baseline *MTADS* magnetometry analysis. A preliminary version of this comparison was attempted in the Fall of 1999 at the Badlands Bombing Range Impact Area.¹⁸ The analysis described

here was able to reject a number of false alarms that would have been marked for digging by the magnetometer analysis. The comparison is incomplete however as there was only one ordnance item detected in the area surveyed by the EM array. A follow-on study is being planned for the Fall of 2001 to provide a better comparison of the cost efficiency of the various analysis strategies. In this Demonstration, an area will be seeded by a third party with ordnance typical of the site and the detection and classification performance of each method will be measured. An addendum will be prepared to this Cost and Performance report to document this comparison.

This page left blank intentionally.

6.0 REFERENCES

1. "Hand-held Gradiometer Survey Test at The Marine Corps Air Ground Combat Center, Twentynine Palms, CA," NAVEODTECHCEN TR, September 1992. This report describes hand-held gradiometer surveys of the MCAGCC Magnetic Test Range conducted by military EOD teams. Their ordnance detection efficiency varied between 25 and 35%.
2. "MTADS TECHEVAL Demonstration, October 1996," H. H. Nelson, J. R. McDonald, and Richard Robertson, NRL/PU/6110--97-348.
3. "Results of the MTADS Technology Demonstration #2, Magnetic Test Range, Marine Corps Air Ground Combat Center, Twentynine Palms, CA, December 1996," J. R. McDonald, H. H. Nelson, R. A. Jeffries, and Richard Robertson, NRL/PU/6110--97-349.
4. "Results of the MTADS Technology Demonstration #3, Jefferson Proving Ground, Madison, IN, January 13-24, 1997," H. H. Nelson, J. R. McDonald, R. A. Jeffries, and Richard Robertson, NRL/PU/6110--99-375.
5. "MTADS Unexploded Ordnance Operations at the Badlands Bombing Range, Pine Ridge Reservation, Cunny Table, SD, July 1997," J. R. McDonald, H. H. Nelson, J. Neece, Richard Robertson and R. A. Jeffries, NRL/PU/6110--98-353.
6. "MTADS Demonstration at the Former Ft. Pierce Amphibious Base, Vero Beach, FL, March 1998," J. R. McDonald, H. H. Nelson, R. A. Jeffries, Richard Robertson, and K. Blankinship, NRL/PU/6110--98-372.
7. "MTADS Live Site Survey, Bombing Target #2 at the Former Buckley Field, Arapahoe County, CO," J. R. McDonald, H. H. Nelson and R. Robertson NRL/PU/6110--99-379.
8. "MTADS Geophysical Survey at The Jamaica Island and Topeka Pier Landfills at The Portsmouth Naval Shipyard, Kittery, ME, October 1998," J. R. McDonald, H. H. Nelson and B. Puc, NRL/PU/6110--99-381.
9. "MTADS Live Site Demonstration, Pueblo of Laguna, 6 July - 7 August 1998," J. R. McDonald, H. H. Nelson and R. A. Jeffries NRL/PU/6110--00-398.
10. "MTADS UXO Survey and Remediation on the Walker River Paiute Reservation, Schurz, NV, November 1998," J. R. McDonald, H. H. Nelson, and R. A. Jeffries NRL/PU/6110--00-406.
11. "MTADS Geophysical Survey of Potential Underground Storage Tank Sites at the Naval District Washington, Anacostia Annex," H. H. Nelson, J. R. McDonald, R. Robertson, and B. Puc, NRL/MR/6110--00-8435.
12. ESTCP Cost and Performance Report. *Multi-Sensor Towed Array Detection System*. September 1999. <http://www.estcp.org/documents/techdocs/199526.pdf>

13. "Collection and Analysis of Multi-sensor Ordnance Signatures with *MTADS*," Bruce Barrow and H. H. Nelson, *J. Environ. Engineering Geophysics*, **3**, 71 (1998).
14. "Model-Based Characterization of EM Induction Signatures for UXO/Clutter Discrimination Using the *MTADS* Platform," Bruce Barrow and H. H. Nelson, Proceedings of the UXO Forum 1999, Atlanta GA, May 25-27, 1999.
15. "Model-Based Characterization of EM Induction Signatures Obtained with the *MTADS* EM Array," Bruce Barrow and H. H. Nelson, *IEEE Trans. Geophys. Remote Sens.*, submitted
16. "Draft Final Removal Report: Ordnance Removal at Army Research Laboratory, Blossom Point Field Test Facility (BPFTF), Blossom Point, Maryland," Human Factors Applications, Inc., DACA87-95-D-0027, Task Order 0008, 18 April 1997.
17. "Electromagnetic Induction and Magnetic Sensor Fusion for Enhanced UXO Target Classification," H. H. Nelson and Bruce Barrow, NRL/PU/6110--00-423.
18. "*MTADS* Unexploded Ordnance Operations at the Badlands Bombing Range Air Force Retained Area, Pine Ridge Reservation, SD, September, 1999," J. R. McDonald, H. H. Nelson, Richard Robertson and R. A. Jeffries, NRL/PU/6110--00-424.

7.0 POINTS OF CONTACT

Dr. Jeffrey Marqusee
ESTCP Director
ESTCP
Telephone: (703) 696-2120
Fax: (703) 696-2114
E-mail: marqusj@acq.osd.mil

Mr. Bill Davis
Explosives Safety Officer
Army Research Laboratory, Blossom Point
Tel: (301) 394-2434
Fax: (301) 394-2514
E-mail: wdavis@arl.mil

Ms. Catherine Vogel
Program Manager, Cleanup
ESTCP
Telephone: (703) 696-2118
Fax: (703) 696-2114
E-mail: vogelc@acq.osd.mil

Mr. Richard Robertson
Program Manager
Hughes Associates, Inc.
Tel: (202) 767-3556
Fax: (202) 404-8119
E-mail: roberts5@ccf.nrl.navy.mil

Dr. Anne Andrews
Analyst
Institute for Defense Analyses
Telephone: (703) 578-2966
Fax: (703) 578-2877
E-mail: Aandres@ida.org

Mr. Larry Koppe
Site Safety Officer
GeoCenters, Inc.
Tel: (301) 753-1690
Fax: (301) 870-3130
E-mail: LarryEOD@aol.com

Dr. Herbert Nelson
Principal Investigator
Naval Research Laboratory
Washington, DC 20375
Tel: (202) 767-3686
Fax: (202) 404-8119
E-mail: herb.nelson@nrl.navy.mil

Dr. Tom Bell
Project Manager
AETC, Inc.
Arlington, VA
Tel: (703) 413-0500
Fax: (703) 413-0505
E-mail: tbell@va.aetc.com

Dr. J. R. McDonald
Deputy Principal Investigator
Naval Research Laboratory
Washington, DC 20375
Tel: (202) 767-3340
Fax: (202) 404-8119
E-mail: j.mcdonald@nrl.navy.mil

Dr. Bruce Barrow
Project Scientist
AETC, Inc.
Arlington, VA
Tel: (703) 413-0500
Fax: (703) 413-0505
E-mail: bjb@va.aetc.com

Mr. Jack Kaiser
Blossom Point Site Manager
Army Research Laboratory, Blossom Point
Tel: (301) 870-2329
Fax: (301) 870-3130
E-mail: jkaiser@arl.mil

This page left blank intentionally.

APPENDIX A

MTADS Target Report from the Final Demonstration.

Target #	Mag Local X (m)	Mag Local Y (m)	Mag Depth (m)	3β Local X (m)	3β Local Y (m)	3β EM Depth (m)	Mag Size (m)	Mag Moment	Hit Quality	β1	β2	β3	Theta	Phi	Psi	χ ²	3β Coherence	Remediation Results
FUS-1	184.40	106.05	0.09	184.34	106.10	0.05	0.037	0.027	0.977	0.78	0.34	0.46	8	-64	-93	1110.4	0.967	Frag
FUS-2	175.73	125.13	0.07	175.57	125.29	0.03	0.035	0.023	0.981	0.39	0.04	0.11	-69	-136	18	808.1	0.969	Frag
FUS-3	164.98	135.15	0.10	164.92	135.18	0.11	0.098	0.515	0.950	1.84	0.31	0.60	-10	123	-41	1349.4	0.968	Frag
FUS-4	158.60	135.47	0.53	158.53	135.49	0.36	0.134	1.312	0.961	10.81	6.77	7.89	20	-171	-121	3841.0	0.988	Frag
FUS-5	170.89	134.25	0.16	170.85	134.38	0.12	0.04	0.035	0.965	1.93	0.54	0.30	11	-168	-117	1306.6	0.965	Non-Ordnance
FUS-6	158.13	145.54	0.45	158.42	145.46	0.37	0.083	0.311	0.943	4.99	1.64	1.86	-31	151	-165	1081.8	0.971	81-mm Mortar
FUS-7	153.48	141.09	0.24	153.76	141	0.11	0.070	0.189	0.943	0.55	0.45	0.39	-30	135	132	651.0	0.948	Ordnance Related
FUS-8	151.64	180.20	0.09	151.70	180.13	0.19	0.026	0.010	0.902	1.79	0.35	0.66	32	107	-34	1268.9	0.964	Frag
FUS-9	138.88	202.80	0.17	138.97	202.79	0.06	0.092	0.427	0.959	0.25	0.17	0.23	-1	-40	-166	305.2	0.950	Non-Ordnance
FUS-10	143.19	120.06	0.12	143.28	120.16	0.14	0.036	0.026	0.962	0.96	0.33	0.62	-3	44	148	1335.6	0.937	Ordnance Related
FUS-11	138.90	163.80	0.08	138.86	163.78	-0.02	0.080	0.279	0.992	0.13	0.03	0.06	-4	-121	-89	70.8	0.949	Frag
FUS-12	142.93	153.88	0.18	143.34	153.86	0.19	0.072	0.206	0.914	0.93	0.17	0.58	-8	26	82	435.8	0.852	Frag
FUS-13	146.36	194.07	0.01	146.13	194.50	0.13	0.032	0.018	0.980	0.80	0.12	0.45	-28	179	87	844.3	0.913	Frag
FUS-14	130.02	163.44	0.50	129.91	163.41	0.48	0.077	0.250	0.967	3.37	1.71	1.55	-63	69	146	504.6	0.972	81-mm Mortar
FUS-15	128.37	154.60	0.07	128.18	155.19	0.09	0.095	0.470	0.993	0.95	0.60	0.29	5	-84	11	967.3	0.940	Frag
FUS-16	132.61	150.66	0.09	132.72	151.07	0.08	0.083	0.311	0.992	0.71	0.04	0.14	-7	53	-95	336.1	0.929	Frag
FUS-17	123.03	132.85	0.10	123.06	132.89	0.02	0.047	0.055	0.898	0.73	0.02	0.07	-24	88	-155	787.4	0.968	Frag
FUS-18	123.87	189.98	0.10	123.77	190.09	0.02	0.031	0.016	0.964	0.32	0.02	0.00	58	-71	-5	355.5	0.965	Frag
FUS-19	124.10	112.56	0.05	124.01	112.57	0.03	0.049	0.062	0.992	0.62	0.03	0.00	4	-163	82	418.2	0.931	Non-Ordnance
FUS-20	116.29	155.73	0.63	116.58	155.89	0.33	0.288	13.033	0.925	12.13	7.03	3.92	-2	62	40	7002.8	0.953	Non-Ordnance
FUS-21	119.36	159.32	0.12	119.30	159.28	0.06	0.035	0.024	0.811	0.67	0.46	0.33	46	-9	83	738.6	0.975	Cone-shaped Warhead
FUS-22	114.89	162.38	0.07	114.87	162.38	0.02	0.029	0.013	0.970	0.21	0.03	0.05	-10	-120	-127	83.3	0.919	Frag
FUS-23	112.19	168.08	0.53	112.18	168.07	0.21	0.342	21.74	0.953	4.41	2.53	1.25	-12	-152	-72	1719.8	0.985	Non-Ordnance
FUS-24	113.05	171.41	0.13	113.12	171.41	0.14	0.044	0.047	0.892	1.67	0.25	0.96	-2	-155	-100	1337.1	0.917	Non-Ordnance
FUS-25	99.69	158.16	0.32	99.69	158.16	0.02			0.971	0.41	0.14	0.01	80	92	106	613.0	0.971	Non-Ordnance
FUS-26	89.48	141.77	0.09	89.55	141.83	0.03	0.033	0.019	0.858	0.45	0.37	0.33	-8	169	-45	477.1	0.982	Ordnance Related
FUS-27	96.67	144.71	0.55	96.97	144.46	0.52	0.082	0.303	0.989	9.02	3.00	5.18	-37	80	-114	1126.0	0.961	Projectile with Frag Sleeve
FUS-28	101.99	148.81	0.49	101.99	148.81	0.19			0.939	0.64	0.04	0.43	-2	70	176	664.6	0.939	Frag
FUS-29	91.48	122.56	0.11	91.5	122.66	0.03	0.037	0.027	0.887	0.30	0.19	0.26	42	20	124	367.5	0.972	Ordnance Related
FUS-30	104.61	109.57	0.16	104.71	109.49	0.13	0.058	0.107	0.906	1.08	0.84	0.70	-10	-37	-13	1398.7	0.964	Ordnance Related
FUS-31	102.79	105.80	0.16	102.7	105.76	0.07	0.060	0.118	0.837	5.08	1.55	1.26	5	30	69	3324.5	0.98	76mmMortar
FUS-32	94.74	102.22	0.66	94.50	102.34	0.36	0.091	0.414	0.981	2.90	1.79	1.25	40	154	-26	590.2	0.969	81-mm Mortar
FUS-33	79.25	96.98	0.13	79.20	97.04	0.08	0.041	0.038	0.939	1.32	0.15	0.19	-2	-77	159	265.7	0.975	Ordnance Related
FUS-34	82.35	109.49	0.11	81.71	109.54	0.17	0.059	0.109	0.948	0.87	0.10	0.06	-23	36	110	260.8	0.929	Frag
FUS-35	78.17	141.27	0.13	77.98	141.26	0.14	0.041	0.036	0.920	0.77	0.54	0.10	-10	95	172	341.9	0.929	Frag

MTADS Target Report from the Final Demonstration (continued).

Target #	Mag Local X (m)	Mag Local Y (m)	Mag Depth (m)	3β Local X (m)	3β Local Y (m)	3β EM Depth (m)	Mag Size (m)	Mag Moment	Fit Quality	β1	β2	β3	Theta	Phi	Ri	χ2	3β Coherence	Remediation Results
FUS-36	76.38	139.16	0.26	76.39	138.96	0.24	0.048	0.060	0.791	1.06	0.24	0.52	-12	-65	-85	250.3	0.928	Frag
FUS-37	79.93	138.19	0.13	79.59	138.34	0.26	0.032	0.019	0.789	1.15	0.56	0.42	-4	-111	180	116.1	0.969	Frag
FUS-38	80.56	141.07	0.41	80.7	141.04	0.22	0.036	0.026	0.829	0.86	0.52	0.17	-16	35	29	197.9	0.956	Frag
FUS-39	76.19	165.19	0.17	76.12	165.24	0.11	0.046	0.052	0.972	1.23	0.23	0.18	6	100	163	517.7	0.962	Frag
FUS-40	81.68	165.59	0.03	81.73	165.57	0.12	0.089	0.388	0.933	0.80	0.41	0.19	-11	77	33	444.1	0.953	Frag
FUS-41	84.51	169.42	0.50	84.51	169.32	0.34	0.264	9.999	0.946	4.97	0.83	1.47	25	-127	-160	806.3	0.95	Non-Ordnance
FUS-42	77.58	179.65	0.54	77.75	179.5	0.39	0.086	0.340	0.963	3.13	1.11	1.67	31	6	166	1248.8	0.95	81-mm Mortar
FUS-43	75.70	178.83	0.12	75.45	179.18	0.29	0.037	0.029	0.857	1.38	0.25	0.45	7	-55	14	359.5	0.915	Non-Ordnance
FUS-44	83.78	181.19	0.45	83.46	181.3	0.40	0.094	0.457	0.939	7.25	1.78	2.56	21	147	57	866.6	0.968	81-mm Mortar
FUS-45	77.82	183.79	0.06	77.81	183.76	0.04	0.071	0.197	0.929	0.32	0.01	0.00	5	-62	-116	115.7	0.935	Frag
FUS-46	59.75	173.51	0.78	59.8	173.75	0.53	0.095	0.467	0.948	4.41	2.55	1.74	54	73	6	239.2	0.986	81-mm Mortar
FUS-47	73.18	153.65	0.24	73.19	153.72	0.12	0.164	2.411	0.965	2.73	1.17	0.39	72	-44	-112	2600.3	0.982	Non-Ordnance
FUS-48	64.93	139.90	0.08	64.87	139.98	0.18	0.032	0.017	0.780	1.52	0.00	0.07	3	-180	-151	419.8	0.938	Frag
FUS-49	73.51	120.40	0.07	73.65	120.42	0.06	0.048	0.061	0.988	1.08	0.13	0.50	-5	117	132	588.2	0.97	Non-Ordnance
FUS-50	67.23	118.92	0.08	67.31	118.89	0.08	0.102	0.574	0.987	0.74	0.05	0.06	14	112	156	381.9	0.937	No Dig Sheet
FUS-51	69.50	94.68	0.06	69.42	94.63	0.08	0.052	0.078	0.989	3.23	0.85	0.42	-1	177	-174	9141.3	0.925	Non-Ordnance
FUS-52	48.17	131.23	0.08	47.98	131.25	0.04	0.027	0.011	0.921	0.36	0.20	0.22	-29	-61	123	244.2	0.954	Frag
FUS-53	46.30	133.26	0.07	46.12	133.16	0.09	0.043	0.043	0.916	1.94	0.45	0.62	14	172	-87	2197.4	0.968	Frag
FUS-54	59.48	152.9	0.05	59.47	152.86	0.11	0.071	0.198	0.977	1.00	0.00	0.07	-1	107	177	452.4	0.921	Non-Ordnance
FUS-55	52.37	164.19	0.74	52.36	164.14	0.18	0.401	35.101	0.944	9.61	3.56	2.43	21	-148	-122	4393.8	0.978	Non-Ordnance
FUS-56	59.91	163.11	0.10	59.9	163.17	0.09	0.026	0.009	0.937	0.59	0.14	0.39	-7	-2	-49	198.8	0.979	Frag
FUS-57	57.82	168.13	0.57	57.84	168.07	0.5	0.091	0.415	0.977	4.91	2.82	2.23	61	-55	77	607.6	0.978	81-mm Mortar
FUS-58	46.54	167.83	0.41	46.49	167.62	0.45	0.104	0.618	0.884	1.97	1.27	0.73	59	-160	32	170.8	0.960	Non-Ordnance
FUS-59	55.48	173.89	0.49	55.47	173.73	0.52	0.076	0.243	0.923	4.06	1.8	2.20	62	44	-90	218.5	0.971	81-mm Mortar
FUS-60	37.47	170.69	0.56	37.37	170.89	0.69	0.076	0.238	0.912	6	2.17	3.38	-59	-37	-108	218.2	0.978	81-mm Mortar
FUS-61	36.59	159.14	0.19	36.55	159.21	0.12	0.103	0.596	0.989	1.19	0.44	0.29	-32	77	-174	867.7	0.964	Frag
FUS-62	43.80	164.26	0.32	43.80	164.26	0.02			0.983	0.21	0	0.02	79	-52	3	230.7	0.983	Nothing Found
FUS-63	51.45	40.57	0.45	51.45	40.63	0.38	0.077	0.243	0.980	5.27	1.12	0.59	33	84	-2	784.4	0.957	81-mm Mortar SEEDED?
FUS-64	77.37	58.42	0.79	76.96	58.67	0.51	0.118	0.886	0.947	11.95	3.27	3.21	8	143	177	1582.0	0.954	4.2" SEEDED
FUS-65	86.33	56.00	0.31	86.33	56.01	0.29	0.101	0.559	0.932	6.62	0.96	1.49	57	115	10	2315.9	0.987	25lb Frag Bomb
FUS-66	86.19	52.41	0.30	86.10	52.46	0.26	0.047	0.058	0.98	2.86	0.26	0.94	3	15	-161	824.8	0.963	2.75" WH SEEDED
FUS-67	105.39	62.43	0.29	105.53	62.32	0.19	0.079	0.269	0.982	1.78	0.91	0.81	72	138	-118	2721.6	0.964	2.75" WH SEEDED
FUS-68	111.13	62.61	0.62	111.08	62.58	0.53	0.066	0.155	0.941	9.42	1.34	1.16	9	48	-101	431.7	0.927	81-mm Mortar SEEDED
FUS-69	124.20	67.11	0.18	124.08	67.16	0.16	0.063	0.133	0.983	4.92	0.63	0.46	-41	32	-71	42666	0.821	MK23 SEEDED
FUS-70	129.70	73.13	0.10	129.61	73.19	0.04	0.036	0.025	0.967	0.44	0.33	0.41	-11	121	90	720.7	0.972	2.75"RktMtr/FinsOpen
FUS-71	68.85	71.7	0.14	68.89	71.66	0.1	0.066	0.155	0.944	3.92	1.43	1.85	-12	-163	-108	2747.3	0.978	81-mm Mortar
FUS-72	182.05	103.38	0.26	182.14	103	0.37	0.083	0.307	0.811	11.79	2.38	3.67	32	-100	-13	8879.9	0.964	81-mm Mortar
FUS-73	168.12	114.9	0.07	167.77	114.62	0.06	0.091	0.409	0.993	0.43	0.29	0.22	0	34	44	352.3	0.968	Frag

MTADS Target Report from the Final Demonstration (continued).

Target #	Mag Local X (m)	Mag Local Y (m)	Mag Depth (m)	3β Local X (m)	3β Local Y (m)	3β EM Depth (m)	Mag Size (m)	Mag Moment	Fit Quality	β1	β2	β3	Theta	Phi	Ri	χ2	3β Coherence	Remediation Results
FUS-74	168.27	145.56	0.10	168.68	145.74	0.26	0.074	0.219	0.97	2.06	1.44	0.95	-6	176	154	1537.9	0.92	No Dig Sheet
FUS-75	151.38	155.44	0.11	151.41	155.67	0.14	0.037	0.028	0.957	0.69	0.49	0.53	-6	-180	10	1028.7	0.942	BOMB FUZE
FUS-76	153.89	145.49	0.32	153.62	145.34	0.38	0.056	0.097	0.866	3.33	1.36	1.4	-11	36	178	776	0.950	Ordnance Related
FUS-77	153.21	158.10	0.30	153.29	157.32	0.19	0.087	0.363	0.945	1.26	0.19	0.5	13	-148	-141	307.1	0.970	Frag
FUS-78	133.95	187.04	0.44	133.95	187.04	0.14			0.986	8.95	2.97	4.95	10	26	79	7499.0	0.986	Non-Ordnance
FUS-79	133.94	191.98	0.37	133.63	191.89	0.44	0.073	0.213	0.956	5.64	1.76	2.82	40	-166	-114	1741.3	0.957	81-mm Mortar
FUS-80	133.99	183	0.66	133.99	183	0.36			0.946	6.93	2.92	1.94	-21	-5	-152	2692.6	0.946	Non-Ordnance
FUS-81	129.53	190.78	0.08	129.33	190.8	0.08	0.080	0.28	0.969	0.34	0.26	0.06	-20	119	166	197.4	0.939	Frag
FUS-82	132.11	195.09	0.35	132.11	195.09	0.05			0.987	0.26	0.09	0.23	62	-11	-120	113.0	0.987	Nothing Found
FUS-83	168.47	99.63	0.14	168.5	99.69	0.09	0.078	0.258	0.955	4.93	1.11	1.29	2	-113	-175	15748	0.953	MORTAR?
FUS-84	166.78	106.86	0.13	166.87	106.96	0.09	0.059	0.109	0.972	0.69	0.11	0.18	-82	158	4	868.2	0.981	Non-Ordnance
FUS-85	164.90	107.62	0.14	164.86	107.61	0.32	0.112	0.765	0.915	6.15	2.01	1.08	13	90	-160	3501.3	0.918	81mmIII Section
FUS-86	165.32	120.7	0.56	165.32	120.7	0.26			0.944	1.46	0.41	1.04	-25	113	-76	562.9	0.944	Frag
FUS-87	165.30	124.12	0.42	165.3	124.12	0.12			0.967	1.05	0.13	0.70	-24	124	170	1616.5	0.967	Frag
FUS-88	149.67	111.73	0.33	149.67	111.73	0.03			0.952	0.62	0.11	0.15	71	24	-69	2960.4	0.952	Ordnance Related
FUS-89	158.99	113.81	0.13	158.71	113.94	0.23	0.037	0.027	0.93	2.20	0.88	1.80	6	173	121	1199.2	0.963	Ordnance Related
FUS-90	157.74	117.69	0.21	158.11	117.53	0.37	0.042	0.04	0.902	2.26	2.04	0.45	20	-31	-24	1220.7	0.888	Frag
FUS-91	160.94	118.81	0.08	160.92	118.92	0.28	0.036	0.025	0.869	2.30	1.19	0.91	17	171	-83	2897.7	0.872	Ordnance Related
FUS-92	161.53	116.61	0.16	161.61	116.61	0.20	0.055	0.091	0.981	6.22	3.04	2.29	-5	-2	-5	6318.0	0.972	81-mm Mortar
FUS-93	149.21	158.38	0.14	149.24	158.33	0.09	0.041	0.036	0.888	0.93	0.22	0.16	-15	13	-44	699.1	0.957	Frag
FUS-94	159.92	164.63	0.02	160.07	164.67	0.05	0.095	0.467	0.932	1.44	0.41	0.44	-9	135	137	1664.7	0.969	Frag
FUS-95	136.68	96.36	0.15	136.75	96.5	0.08	0.041	0.037	0.967	0.71	0.34	0.18	16	99	-137	848.1	0.920	2.75"RktMtr
FUS-96	136.14	101.52	0.08	136.07	101.48	0.17	0.059	0.112	0.915	5.67	3.00	2.67	-10	28	-124	7030.2	0.981	Recoilless Rifle Round 76-80mm/18"
FUS-97	137.75	149.22	0.13	137.83	149.16	0.17	0.052	0.075	0.940	2.70	1.28	0.96	-12	100	175	4276.5	0.939	Ordnance Related
FUS-98	138.74	147.83	0.25	138.5	147.65	0.39	0.148	1.747	0.960	4.83	0.25	0.35	6	95	113	599.5	0.924	Frag
FUS-99	137.71	146.32	0.19	137.4	146.24	0.09	0.043	0.044	0.747	0.65	0.22	0.05	-62	-52	108	1862.2	0.958	Frag
FUS-100	138.32	143.45	0.32	138.55	143.38	0.27	0.045	0.048	0.619	1.59	0.38	1.02	33	17	-77	648.4	0.938	Ordnance Related
FUS-101	140.33	175.3	0.07	140.3	175.27	0.13	0.090	0.397	0.997	0.47	0.02	0.12	5	-165	110	155.9	0.888	Frag
FUS-102	133.83	171.49	0.09	134.22	172.19	0.23	0.059	0.113	0.933	1.14	0.56	1.10	11	85	-100	500.0	0.945	Frag
FUS-103	137.26	191.92	0.13	137.26	191.87	0.18	0.065	0.152	0.985	3.30	1.51	0.84	20	81	-168	2616.2	0.975	Non-Ordnance
FUS-104	138.56	191.62	0.2	138.33	191.7	0.24	0.036	0.026	0.948	2.51	0.93	1.42	-13	-3	170	2155.4	0.966	60mmMortar
FUS-105	136.68	189.81	0.26	136.7	189.87	0.24	0.062	0.132	0.960	5.65	1.53	1.13	18	36	41	2210.2	0.986	81-mm Mortar
FUS-106	132.99	85.46	0.28	132.97	85.37	0.28	0.100	0.539	0.992	1.15	0.18	0.00	-50	56	113	744.1	0.928	Frag
FUS-107	126.83	94.48	0.54	126.76	94.45	0.45	0.243	7.832	0.859	189.02	45.23	89.93	2	-178	-77	815158	0.918	5"Rkt
FUS-108	124.10	96.01	0.13	124.14	96.06	0.04	0.032	0.017	0.761	5.3	1.40	3.62	-45	119	127	71941	0.972	Non-Ordnance
FUS-109	130.87	112.16	0.40	131.36	112.59	0.07	0.110	0.728	0.693	7.47	1.98	2.02	-4	86	-47	21118.2	0.963	Frag
FUS-110	123.26	123.52	0.11	123.32	123.36	-0.01	0.041	0.036	0.94	0.25	0.15	0.20	9	-104	-123	451.4	0.950	Ordnance Related

MTADS Target Report from the Final Demonstration (continued).

Target #	Mag Local X (m)	Mag Local Y (m)	Mag Depth (m)	3β Local X (m)	3β Local Y (m)	3β EM Depth (m)	Mag Size (m)	Mag Moment	Fit Quality	β1	β2	β3	Theta	Phi	Ri	χ2	3β Coherence	Remediation Results
FUS-111	129.01	123.99	0.21	128.91	124.09	0.16	0.072	0.200	0.922	0.92	0.20	0.73	5	130	-85	537.7	0.916	Frag
FUS-112	125.64	136.44	0.28	125.55	136.46	0.26	0.037	0.028	0.861	2.16	1.63	1.16	-55	101	-122	1391.3	0.980	81-mm Mortar
FUS-113	128.76	136.3	0.11	128.69	136.25	0.10	0.042	0.041	0.925	0.47	0.34	0.26	-6	-10	-152	253.5	0.973	Non-Ordnance
FUS-114	123.54	162.86	0.22	123.5	162.74	0.17	0.103	0.585	0.936	4.18	0.65	0.56	1	72	-180	1404.7	0.966	Non-Ordnance
FUS-115	130.77	175.56	0.35	130.61	175.46	0.37	0.080	0.276	0.98	5.86	2.51	2.89	55	-163	117	1657.1	0.980	No Dig Sheet
FUS-116	122.95	175.89	0.08	122.84	175.9	0.27	0.040	0.035	0.986	3.75	0.57	0.31	2	-95	-9	1539.8	0.897	Non-Ordnance
FUS-117	119.33	166.90	0.44	119.51	166.9	0.37	0.087	0.352	0.958	7.60	2.00	3.20	33	-24	-143	6522.1	0.955	81-mm Mortar
FUS-118	123.23	168.45	0.11	122.88	168.73	0.12	0.018	0.003	0.707	0.65	0.21	0.20	37	-124	-103	592.7	0.941	Frag
FUS-119	126.29	197.71	0.05	126.35	197.51	0.06	0.041	0.038	0.888	0.92	0.27	0.29	7	2	-46	427.6	0.965	Ordnance Related
FUS-120	133.84	204.27	0.09	133.88	204.32	0.11	0.051	0.074	0.968	0.58	0.38	0.28	41	165	120	398.5	0.970	Ordnance Related
FUS-121	113.27	78.31	0.17	113.62	78.29	0.27	0.061	0.122	0.877	1.77	0.33	0.20	1	-163	-12	340.4	0.905	Non-Ordnance
FUS-122	108.73	88.75	0.18	108.77	88.79	0.15	0.064	0.142	0.894	5.02	2.01	2.10	-3	57	-171	6490.4	0.979	81-mm Mortar
FUS-123	111.67	100.19	0.11	111.51	100.22	0.13	0.087	0.355	0.902	0.84	0.26	0.48	-6	85	114	851.3	0.900	Frag
FUS-124	118.45	106.53	0.55	118.57	106.59	0.42	0.082	0.300	0.957	3.62	1.52	2.10	54	46	44	593.6	0.981	81-mm Mortar
FUS-125	120.26	112.66	0.12	120.33	112.83	0.26	0.042	0.039	0.932	1.66	0.68	1.05	-7	-99	102	841.9	0.901	Ordnance Related
FUS-126	113.56	132.65	0.1	113.2	133.16	0.06	0.041	0.037	0.967	0.75	0.25	0.07	-73	43	-145	1025.2	0.976	Frag
FUS-127	106.36	134.57	0.11	106.34	134.66	0.22	0.084	0.321	0.792	1.08	0.05	0.06	-6	1	-56	387.6	0.868	Frag
FUS-128	120.67	135.58	0.11	120.66	135.43	0.34	0.064	0.143	0.91	3.05	0.04	0.16	-5	-110	1	802.8	0.859	Non-Ordnance
FUS-129	109.89	153.8	0.47	109.86	153.77	0.12	0.272	10.942	0.897	3.46	1.89	0.71	9	-121	101	4377.4	0.973	Non-Ordnance
FUS-130	111.49	163.56	0.27	111.42	163.58	0.18	0.066	0.153	0.983	4.57	1.83	1.35	-21	13	-50	2929.1	0.983	81-mm Mortar
FUS-131	108.55	164.24	0.37	108.68	164.37	0.42	0.060	0.120	0.660	4.09	1.76	2.99	-44	126	-60	319.0	0.985	81-mm Mortar
FUS-132	115.74	167.11	0.09	115.69	167.02	0.09	0.061	0.122	0.983	3.66	0.78	2.16	-5	-2	-107	5265.1	0.971	Non-Ordnance
FUS-133	89.84	190.89	0.10	89.7	190.91	0.13	0.082	0.299	0.985	1.26	0.61	0.41	5	74	0	776.5	0.954	60mmMortar
FUS-134	88.15	184.29	0.06	88.15	184.31	-0.04	0.085	0.331	0.981	0.14	0.00	0.01	-7	-18	-38	51.9	0.926	Frag
FUS-135	91.05	177.83	0.04	91.11	177.85	0.06	0.049	0.063	0.984	1.46	0.70	0.27	8	-91	-17	660.7	0.978	Frag
FUS-136	91.11	175.62	0.12	90.88	175.14	0.06	0.071	0.198	0.957	0.28	0.10	0.23	27	66	127	281.1	0.959	Frag
FUS-137	93.82	174.63	0.59	93.88	174.45	0.27	0.337	20.752	0.956	4.66	1.31	2.46	34	-118	25	3925.3	0.961	Non-Ordnance
FUS-138	94.64	172.09	0.01	94.71	172.17	0.11	0.042	0.039	0.783	2.48	1.87	1.43	8	-87	-23	3358.2	0.968	81 mm Nose Section
FUS-139	96.03	178.16	0.24	95.25	177.14	0.30	0.095	0.466	0.703	5.31	2.14	1.29	8	-18	24	2296.5	0.933	Frag
FUS-140	101.05	171.69	0.25	100.98	171.81	0.22	0.154	1.983	0.988	17.28	9.43	13.14	-45	-24	-118	135963	0.968	Frag
FUS-141	94.33	158.52	0.13	94.35	158.42	0.17	0.075	0.227	0.981	0.93	0.35	0.22	44	-58	-1	1256.7	0.946	Frag
FUS-142	90.06	157.56	0.65	90.08	157.5	0.35	0.357	24.791	0.970	9.33	2.85	1.71	-4	-171	-72	1929.7	0.971	Non-Ordnance
FUS-143	86.70	157.14	0.30	86.81	157.39	0.30	0.084	0.317	0.986	6.46	1.98	0.91	-42	-124	138	1979.0	0.985	81-mm Mortar
FUS-144	92.85	157.30	0.11	92.71	156.53	0.02	0.064	0.143	0.917	0.47	0.02	0.07	47	-88	148	1563.3	0.948	Frag
FUS-145	96.22	151.97	0.53	96.08	152.07	0.30	0.329	19.35	0.977	10.73	2.71	3.75	10	-36	166	3283.4	0.970	Non-Ordnance
FUS-146	94.98	119.88	0.42	94.88	119.51	0.63	0.058	0.104	0.893	14.51	3.98	1.43	30	-86	34	3184.2	0.929	81-mm Mortar
FUS-147	96.13	122.24	0.09	96.07	122.16	0.15	0.050	0.066	0.836	2.94	1.20	2.03	12	-59	-68	5986.2	0.911	BombFuze
FUS-148	91.29	117.57	0.75	90.92	117.31	0.98	0.130	1.187	0.968	48.84	14.22	6.10	27	-115	-133	1096.4	0.948	105mmPlusScrap

MTADS Target Report from the Final Demonstration (continued).

Target #	Mag Local X (m)	Mag Local Y (m)	Mag Depth (m)	3β Local X (m)	3β Local Y (m)	3β EM Depth (m)	Mag Size (m)	Mag Moment	Fit Quality	β1	β2	β3	Theta	Phi	Ri	χ2	3β Coherence	Remediation Results
FUS-149	95.12	115.82	0.20	94.66	115.95	0.14	0.049	0.066	0.800	0.73	0.14	0.33	63	-172	-68	996.4	0.963	Frag
FUS-150	97.11	109.69	0.29	97.11	109.74	0.34	0.075	0.226	0.875	3.89	2.26	3.27	16	121	109	2661.4	0.943	4.2" Broke in Half
FUS-151	97.63	94.7	0.02	97.54	94.72	0.07	0.057	0.098	0.850	4.45	1.42	1.69	10	62	126	9741.1	0.967	Frag
FUS-152	105.68	90.28	0.08	105.17	90.29	0.05	0.108	0.688	0.974	1.25	0.84	1.00	69	-7	-48	3833.6	0.971	Frag
FUS-153	92.88	72.93	0.22	92.89	72.68	0.29	0.078	0.257	0.829	3.76	2.15	2.03	30	12	66	1540.5	0.978	81-mm Mortar
FUS-154	78.77	71.03	0.10	78.85	71.06	0.01	0.074	0.224	0.907	6.10	2.61	1.76	9	-97	-154	22986.3	0.984	81 mmillum
FUS-155	81.02	76.06	0.19	81.05	76.19	0.19	0.083	0.315	0.943	4.66	2.28	1.41	42	33	170	11688.7	0.958	81-mm Mortar
FUS-156	74.53	70.36	0.21	74.59	70.29	0.23	0.062	0.132	0.953	6.79	3.69	2.35	4	167	16	15916.3	0.925	81-mm Mortar
FUS-157	76.18	72.49	0.09	76.16	72.55	0.12	0.045	0.049	0.977	3.2	1.44	0.6	1	54	-161	5657.4	0.936	Frag
FUS-158	84.51	86.96	0.17	84.59	86.91	0.13	0.032	0.018	0.964	2.01	0.51	0.86	-3	141	-91	1186.9	0.969	Frag
FUS-159	82.38	118.97	0.48	82.28	118.92	0.42	0.085	0.333	0.948	3.71	2.02	2.44	-52	9	92	654.3	0.983	81-mm Mortar
FUS-160	79.13	114.53	0.45	78.86	114.35	0.47	0.070	0.186	0.906	5.17	1.93	2.60	43	-92	-93	1499.7	0.962	81-mm Mortar
FUS-161	83.50	142.28	0.56	83.71	142.17	0.43	0.085	0.330	0.967	7.97	2.09	3.22	27	-12	58	2417.7	0.954	81-mm Mortar
FUS-162	77.86	167.73	0.35	77.86	167.73	0.05			0.977	0.28	0.19	0.25	35	-128	160	164.6	0.977	Ordnance Related
FUS-163	75.37	173.65	0.12	75.3	173.86	0.05	0.045	0.049	0.827	0.86	0.54	0.70	16	55	44	803.8	0.976	Ordnance Related
FUS-164	83.62	173.63	0.78	83.95	173.19	0.86	0.332	19.82	0.886	41.23	0.00	40.33	-42	-116	44	10115.4	0.926	Non-Ordnance
FUS-165	74.88	182.53	0.64	74.73	182.7	0.41	0.073	0.212	0.905	3.91	0.53	1.62	8	-111	-10	1346.3	0.907	81-mm Mortar
FUS-166	74.38	187.01	0.45	74.48	187.21	0.69	0.088	0.366	0.981	3.45	1.68	1.61	71	26	85	723.00	0.985	81-mm Mortar
FUS-167	81.47	186.46	0.42	81.82	186.88	0.65	0.055	0.092	0.947	10.54	3.16	1.69	9	49	-58	695.7	0.915	81-mm Mortar
FUS-168	83.42	188.39	0.55	83.52	188.68	0.84	0.293	13.672	0.941	28.63	2.85	0.00	54	45	122	11281.8	0.889	Non-Ordnance
FUS-169	63.84	185.26	0.56	63.88	185.31	0.47	0.077	0.250	0.973	2.85	1.98	1.57	59	-70	-56	240.6	0.989	81-mm Mortar
FUS-170	64.40	183.25	0.38	64.39	183.12	0.42	0.067	0.165	0.950	7.23	2.62	2.11	26	-74	49	1755.0	0.970	81-mm Mortar
FUS-171	66.42	182.07	0.51	66.75	182.18	0.75	0.073	0.215	0.981	4.8	0.78	1.53	35	151	114	314.0	0.969	81-mm Mortar
FUS-172	58.50	170.57	0.25	60.68	170.58	0.58	0.244	7.842	0.772	8.29	3.11	2.13	-30	175	-148	592.3	0.967	Frag
FUS-173	62.97	170.42	0.09	62.96	170.35	0.11	0.124	1.026	0.731	3.94	1.13	0.54	-6	-127	155	1957.3	0.978	Frag
FUS-174	67.74	168.10	0.48	67.6	167.98	0.37	0.112	0.769	0.950	8.08	2.41	4.68	36	-117	-164	2574.6	0.983	81-mm Mortar
FUS-175	65.69	157.17	0.04	65.65	157.21	0.11	0.036	0.025	0.792	0.97	0.73	0.55	12	99	174	1076.1	0.966	Frag
FUS-176	71.00	159.89	0.33	71.37	159.62	0.47	0.070	0.185	0.962	5.60	2.19	1.69	30	-51	-137	823.1	0.976	Frag
FUS-177	60.18	151.02	0.01	60.19	151	0.02	0.039	0.033	0.994	0.74	0.11	0.07	-3	-149	-177	752.4	0.945	Non-Ordnance
FUS-178	61.22	130.56	0.59	61.15	129.97	0.93	0.080	0.283	0.943	4.90	1.20	4.28	68	-122	-179	357.0	0.971	81-mm Mortar?
FUS-179	63.00	127.23	0.16	63.1	127.31	0.11	0.068	0.171	0.972	0.58	0.05	0.24	50	121	-159	960.4	0.957	Frag
FUS-180	60.93	116.11	0.63	60.8	116.24	0.40	0.098	0.512	0.947	3.97	2.37	1.20	23	124	-124	957.8	0.971	81-mm Mortar
FUS-181	67.45	88.93	1.17	67.98	89.09	1.17	0.180	3.157	0.948	168.06	60.27	52.22	-6	32	-144	4173.4	0.931	8Venturies
FUS-182	70.63	88.05	0.15	70.68	88.08	0.13	0.071	0.193	0.967	7.11	2.96	2.39	-6	-114	22	26947.1	0.949	81-mm Mortar
FUS-183	71.12	85.62	0.37	71.09	85.64	0.36	0.270	10.704	0.846	106.81	11.72	31.51	-4	58	-6	914831	0.869	Non-Ordnance
FUS-184	75.91	86.17	0.40	75.57	86.52	0.68	0.115	0.830	0.888	10.69	6.42	9.08	40	21	-97	1177.4	0.968	Frag
FUS-185	77.42	84.72	0.45	77.59	84.75	0.20	0.121	0.955	0.763	10.73	4.40	8.3	9	80	-101	42512.9	0.945	81-mm Mortar
FUS-186	55.71	132.81	0.48	55.28	132.81	0.39	0.086	0.342	0.917	5.59	1.98	1.45	50	-154	106	1419.2	0.983	81-mm Mortar

MTADS Target Report from the Final Demonstration (continued).

Target #	Mag Local X (m)	Mag Local Y (m)	Mag Depth (m)	3β Local X (m)	3β Local Y (m)	3β EM Depth (m)	Mag Size (m)	Mag Moment	Fit Quality	β1	β2	β3	Theta	Phi	Si	χ2	3β Coherence	Remediation Results
FUS-187	45.62	146.87	0.14	45.69	146.82	0.07	0.067	0.163	0.981	5.24	1.04	1.68	-13	132	-128	42751.7	0.922	Non-Ordnance
FUS-188	55.82	143.67	0.77	55.72	143.8	0.47	0.125	1.067	0.951	5.69	4.06	2.07	63	93	-20	999.3	0.978	15-25FragBomb
FUS-189	54.79	150.73	0.42	54.86	150.67	0.34	0.089	0.383	0.977	6.32	2.48	1.51	40	-5	29	7431.4	0.948	81-mm Mortar
FUS-190	50.89	140.98	0.12	50.77	141.02	0.15	0.029	0.014	0.838	1.39	0.37	0.49	0	-2	-129	457.5	0.966	Non-Ordnance
FUS-191	46.75	159.7	0.17	46.77	159.72	0.10	0.103	0.593	0.975	0.74	0.13	0.26	17	125	-96	227.4	0.957	Frag
FUS-192	51.15	179.35	0.50	51.31	179.58	0.43	0.077	0.249	0.936	4.91	1.90	2.21	15	38	-171	381.0	0.984	81-mm Mortar
FUS-193	50.45	170.94	0.57	50.45	170.94	0.27			0.981	2.06	0.62	0.91	36	2	22	195.3	0.981	60mmM720
FUS-194	44.21	175.55	0.60	44.13	175.3	0.52	0.074	0.217	0.957	3.96	0.50	1.73	42	-46	172	612.2	0.954	81mm HE M371
FUS-195	45.83	172.3	0.55	45.71	172.28	0.53	0.073	0.214	0.961	3.13	1.47	2.59	-49	149	-170	342.4	0.974	81-mm Mortar
FUS-196	40.04	176.63	0.07	40.01	176.76	0.21	0.036	0.025	0.798	2.61	1.17	1.63	11	-35	66	1977.6	0.967	Frag
FUS-197	35.78	175.99	0.36	35.87	176.09	0.50	0.061	0.124	0.928	5.57	3.77	2.31	37	-2	-31	604.1	0.975	81-mm Mortar
FUS-198	29.47	176.71	0.33	29.59	176.63	0.37	0.057	0.101	0.958	5.9	2.84	4.43	-26	146	-91	1589.6	0.978	81-mm Mortar
FUS-199	41.30	51.76	0.45	41.38	51.93	0.71	0.085	0.331	0.959	14.02	2.06	5.82	61	-20	166	9362.6	0.817	81-mm Mortar
FUS-200	49.44	48.31	0.17	49.43	48.45	0.23	0.050	0.066	0.939	4.02	0.34	0.66	-2	-78	-116	1604.4	0.931	MK23 SEEDED
FUS-201	90.08	67.3	0.82	90.01	67.52	0.56	0.115	0.828	0.979	5.85	1.61	4.69	6	154	-32	1296.1	0.946	105mm SEEDED



ESTCP Program Office

**901 North Stuart Street
Suite 303
Arlington, Virginia 22203
(703) 696-2117 (Phone)
(703) 696-2114 (Fax)
e-mail: estcp@estcp.org
www.estcp.org**